**Astronomy
& Astrophysics**

Hypersonic collision of a blast wave on a low-mass star

D. García-Senz[1,2], N. Serichol[1], and E. Bravo[1,2]

[1] Departament de Física i Enginyeria Nuclear, UPC, Sor Eulàlia d'Anzizu s/n, B5, 08034 Barcelona, Spain
e-mail: domingo.garcia@upc.es; nuria.serichol@upc.es; eduardo.bravo@upc.es
[2] Institut d'Estudis Espacials de Catalunya, Gran Capità 2-4, 08034 Barcelona, Spain

Abstract. When a neutron star is born as a result of the accretion-induced collapse (AIC) of a white dwarf, a small but significant fraction of its mass can be simultaneously expelled at a velocity of around 10^4 km s^{-1}. In this paper we study the collision between the gas ejected during the AIC of a white dwarf and a 0.3 $M_\odot$ main-sequence star by using numerical simulation techniques. We found that, for a plausible combination of the orbital parameters and impact energy, the low-mass star is completely destroyed. This scenario can help to explain the origin of isolated millisecond pulsars.

Key words. hydrodynamics – stars: supernovae: general – stars: pulsars: general

1. Introduction

The issue of the origin of millisecond pulsars (MSP) has not yet been satisfactorily settled. The favoured models assume that MSP are the endpoint product of low-mass X-ray binary evolution. In these models a persistent phase of accretion near the Eddington limit, which causes the X-ray emission, would also be responsible for the ultra-short spin of the pulsar (Bhattacharya 1996).

Another proposed model relies on the accretion-induced collapse of a white dwarf. The starting configuration is a binary system composed of a massive white dwarf, the primary ($M_1 \geq 1.1\ M_\odot$), and a secondary star (either evolved or unevolved) which come close enough as to allow the exchange of matter through the inner Lagrangian point. Under the appropriate conditions (mass accretion rate, initial configuration of the system) the white dwarf would retain a fraction of the accreted matter, then approaching the Chandrasekhar mass limit to finally collapse to a neutron star (Canal et al. 1990). As a consequence of accretion, the former white dwarf also increases its angular velocity. Conservation of angular momentum during the collapse would give rise to a millisecond pulsar. As the implosion process is thought to be rather quiet, the binary system has a good chance of surviving in the end.

If the origin of MSP is still vividly debated, the isolated existence of a handful of them is even more intriguing. In order for them to fit into the scenarios described above, the key question is how to get rid of the secondary once the MSP has formed. Nowadays the most popular model invokes the ionization of the secondary by the radiation of the pulsar (Ruderman et al. 1989). These models are supported by the observation of a few pulsars, such as PSR 1957+20, which have very low-mass orbiting companions close enough to be heavily irradiated. Nevertheless, there is no wide agreement and some authors claim that this mechanism is not powerful enough to destroy the secondary (Ryba & Taylor 1991).

On the other hand, the AIC scenario could provide a natural way of removing the secondary by direct interaction with the gas ejected during the implosion. Unfortunately, several calculations carried out in the past showed that, both for a main-sequence star of 1 $M_\odot$ and for a red giant star of similar mass, even the powerful blast wave caused by a type Ia supernova explosion is not able to blow away the secondary. It would be extremely difficult to shatter any secondary unless it had both a relatively large radius and a low binding energy. Almost two decades ago, Iben & Tutukov (1984) speculated that the collision of 0.1 $M_\odot$ of gas ejected during the AIC process, and moving near the escape velocity, would be enough to destroy an unevolved star with $M_2 = 0.3\ M_\odot$. The *main aim* of this paper is to discern whether or not the collision of such a stream of gas would destroy the low-mass secondary in the aforementioned conditions. The calculations were carried out in three dimensions using a smoothed-particle hydrodynamics (SPH) code. The orbit of the secondary is included for the first time in the simulation of the impact. To some extent our work complete that already done by Fryxell & Arnett (1981), Livne et al. (1992) and, very recently, by Marietta et al. (2000), which considered

---

Send offprint requests to: D. García-Senz
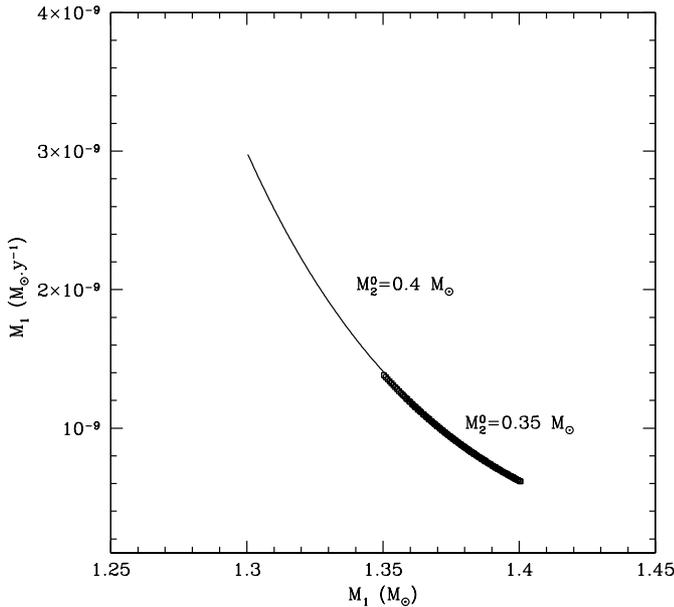
Fig. 1. Evolution of the accretion rate as a function of the instantaneous mass of the white dwarf for two cases: $M_1^0 = 1.3\ M_\odot$, $M_2^0 = 0.4\ M_\odot$ (continuum line), and $M_1^0 = 1.35\ M_\odot$, $M_2^0 = 0.35$ (thick line)

a different kind of secondary star. In Sect. 2 we explain the details of the initial configuration of our system and the relevant features of the method of calculation. The evolution of the collision is presented in Sect. 3 and, finally, our conclusions are summarized in Sect. 4.

2. Initial configuration and method of calculation

In the following we will assume that a compact binary system consisting of a white dwarf of about $1.3\ M_\odot$, composed of oxygen, neon and magnesium, plus a secondary of 0.35–$0.4\ M_\odot$ has come into being after one or two non-conservative mass-loss episodes in previous common envelope stages (see Sect. 4 for a brief discussion). Let us also assume that the orbiting radius is small enough to keep the Roche lobe of the secondary M_2, in contact with its outer surface. Hence, for a given mass and radius of the secondary the orbital separation and orbital velocity can be inferred. Then, the accretion rate can be approximated by (Ritter 1985):

$$\dot{M}_1 = [r_{g_1}^2 R_1^2 M_1 \Omega_1 - \dot{J}_{\text{syst}}] \left\{ \frac{G^{2/3}[(5+3\alpha_2)M_1 - 6M_2]}{6(M_1+M_2)^{1/3}\omega^{1/3}} \right.$$
$$\left. + r_{g_2}^2 R_2^2 \omega \frac{\alpha_2+3}{2} - r_{g_1}^2 R_1^2 \Omega_1 (1+2\alpha_1) \right\}^{-1} \quad (1)$$

where $M_i, R_i\ i = 1, 2$ refer to mass and radius of the primary and secondary respectively, and $r_{g_i}, \Omega_i, \alpha_i, \dot{J}_{\text{syst}}$ and ω are the gyration radius, spin angular frequency, mass-radius exponent, systemic loss of angular momentum and orbital angular frequency respectively. Two sources of loss of angular momentum have been considered: gravitational

wave radiation (Landau & Lifshitz 1987) and magnetic braking (Patterson 1984). Given the appropriate initial conditions (here $M_1^0 = 1.35, 1.30\ M_\odot$, $M_2^0 = 0.35, 0.4\ M_\odot$, $R_2^0 = 0.56, 0.54\ R_\odot$ respectively, and $\Omega_1 = 0, \Omega_2 = \omega$) and supposing that the flowing matter is accreted through a Keplerian disc with internal radius R_1, transferring part or all of its angular momentum to the white dwarf, we can roughly track the evolution of the primary prior to collapse. The mass-radius relationship for the white dwarf is taken from Nauenberg (1972) and is $R_2 \propto M_2^{-1/3}$ for the convective secondary. As can be seen in Fig. 1, the resulting accretion rate decreases with time from few times $10^{-9}\ M_\odot\ \text{yr}^{-1}$ to $5\ 10^{-10}\ M_\odot\ \text{yr}^{-1}$. According to Nomoto & Kondo (1991), such a slow rate would lead to the collapse of the star provided its initial mass is higher than $\simeq 1.3\ M_\odot$, otherwise the nova-like phenomenon would prevent mass growth of the white dwarf. This leaves white dwarfs composed of oxygen, neon and magnesium as the only candidates for collapse (Gutiérrez et al. 1996). For example, for an $M_1^0 = 1.35\ M_\odot$ star, it would take about 50 Myr to accumulate enough material to reach $1.4\ M_\odot$ and ensure the implosion of the primary. At that moment the secondary mass would be $M_2 \simeq 0.3\ M_\odot$ and it would be orbiting at $2.3\ R_\odot$ from the nascent neutron star with a period of 0.34 days. Conservation of the angular momentum, gained by the white dwarf during the accretion process, will give rise to a pulsar spinning at a millisecond level after the implosion. The actual value of the mass ejected during the collapse of the white dwarf is not known but it is thought to be between zero and a few tenths of solar masses. The impacting velocity has been taken to be close to the escape velocity, around $10\,000\ \text{km s}^{-1}$. This configuration, summarized in Table 1, represents the starting point of our simulations.

It is well known that low-mass stars have large convective envelopes. In fact, for a $0.3\ M_\odot$ star, the whole interior is convective and its structure can be approximated by a $n = 3/2$ polytrope, which is less centrally condensed than a radiative type $n = 3$ polytrope of the same mass. Thus, low-mass stars have a higher concentration of matter near the surface, which is where the ablation takes place in our scenario, being easier to destroy than more massive stars. Equilibrium models for these stars have recently been calculated by Chabrier & Baraffe (1997). We have fitted one of their models with $M = 0.3\ M_\odot$ by an $n = 3/2$ polytrope (Fig. 2). The resulting structure was mapped to a three-dimensional distribution of $22\,400$ particles of equal mass. A wedge was taken from the spherical ejecta with size twice the radius of the secondary and thickness of one-third of the orbital separation (Colgate 1970). The density profile inside the ejecta follows a power-law distribution $\rho \propto r^n$ ($n = -6$), and a homologous expansion rate $v \propto r$, which is more realistic than the flat profile considered in most of the previous works dealing with collisions. Given the total kinetic energy of the gas (here, the specific kinetic energy was $E_k = 0.5\ 10^{18}\ \text{erg g}^{-1}$), this resulted in a velocity range from $7900\ \text{km s}^{-1}$ in the innermost part of

Table 1. Input parameters for the initial model[a]

$M_2(M_\odot)$	$R_2(R_\odot)$	ρ_c (gr cm^{-3})	a ($R_\odot$)	Period (days)	$\bar{v}_{\rm ej}$ (km s^{-1})	$M_{\rm in}(M_\odot)$	$p_{\rm in}$ (g cm s^{-1})	$E_{\rm Kin}/E_{\rm B}$
0.3	0.594	12	2.3	0.34	1.0 10^4	1.7 10^{-3}	3.4 10^{39}	7.5

[a] The parameters are: mass, radius and central density of the secondary, orbital separation, period, rms velocity of the ejecta, incident mass, incident momentum and ratio between the incident kinetic energy and the binding energy of the secondary respectively.
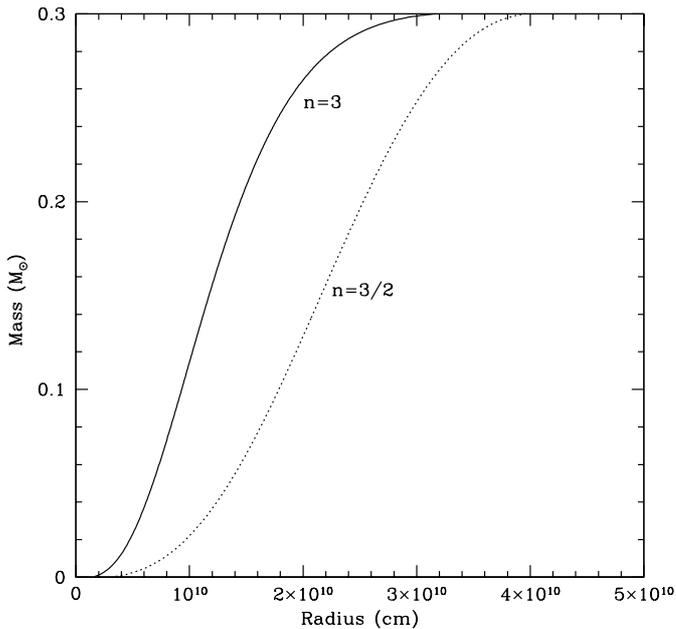
Fig. 2. Mass distribution for polytropes of index $n = 3/2$ and $n = 3$ with total mass 0.3 $M_\odot$

the shell to $14\,200$ km s^{-1} at the outer edge. The number of mass points in the chunk of the ejecta was 2200.

The interaction between the hypersonic ejecta and the secondary was simulated using a SPH code. The orbital dynamics (spin of the secondary and orbital rotation) was also incorporated into the simulation in order to take into account the gravitational attraction onto the ablated matter, due to the 1.3 $M_\odot$ neutron star. The tidal torques produced by the neutron star could be specially relevant in determining the stability of the perturbed-expanded-secondary. The features of the particle hydrocode are fairly standard (Hernquist & Katz 1989) and do not warrant further explanation. Gravitation was calculated by means of a multipolar expansion, retaining up to the quadrupole term. The included physics is simple: the equation of state is that of an ideal gas of ions and electrons plus radiation. Shocks were handled by using the SPH form of the artificial viscosity. The secondary was composed entirely of hydrogen whereas the ejecta was composed of oxygen, neon and magnesium.

To test the stability of the initial configuration a model consisting of a static point mass of 1.3 $M_\odot$ and an orbiting secondary of 0.3 $M_\odot$ was run prior to the simulations given

in Table 1. We followed one complete orbit, during which the trajectory of the secondary remained circular. No mass loss was observed during the evolution in spite of the tidal deformation of the secondary and the numerical noise.

3. Results of the simulation

As can be seen in Table 1, there is a large ratio between the incident kinetic energy and the binding energy of the secondary. Therefore, even a low shock efficiency could lead to the total or partial disruption of the star. As was pointed out in previous calculations (i.e. Fryxell & Arnett 1981), the effect of the supersonic collision is twofold. First, the direct momentum transfer from the gas to the star strips a portion of the envelope of the secondary, also giving a radial velocity component of a few dozens of kilometres per second to the remnant. Second, the energy deposition which takes place in this inelastic collision ablates part of the envelope and heats the core.

The evolution of the interaction is summarized in the nine snapshots shown in Fig. 5. According to the simulation, the process can be roughly separated into four stages, represented by four limiting times:

1) $t_1 \leq 50$ s: this is the time taken by the ejecta to move a distance equal to its own width. During this period there is an inelastic collision with the envelope of the star, in which the incoming flow of gas transforms its kinetic energy into internal:

$$\frac{1}{2}v_{ej}^2 = \int C_v \mathrm{d}T - \int P\frac{\mathrm{d}\rho}{\rho^2}. \qquad (2)$$

The initial specific kinetic energy is in this way stored basically in the radiation field. According to our simulation, the density increased by a factor thirty while the temperature rose to $\simeq 7\,10^7$ K, which was not high enough to allow any substantial combustion of the hydrogen in the scale of time considered. The outermost stellar material was also compressed and heated. The overpressure gave rise to a *shock wave* which began to move towards the centre of the secondary.

2) $t_2 \leq 150$ s: this is the time taken by the ejecta to cross the secondary. The flow of gas wrapped around the low-mass star until it finally went out and the interaction ceased. A fraction of the outermost zone ($\simeq 4\%$ of the total mass of the secondary) was stripped during the interaction, becoming unbound and leaving the star. On the other hand, part of the impacting gas reversed its velocity and moved back towards the neutron star.

3) $t_3 \leq 1200$ s: this is roughly the time necessary for the induced shock to move a distance equal to the diameter of the secondary. The propagation of the shock is depicted in Fig. 3, in which the density jump is shown at four different times. By dividing the distance between the second and fourth peaks, at $t = 149$ s and $t = 457$ s respectively, by the elapsed time we got an average shock velocity of $D = 3.9 \ 10^7$ cm s^{-1}, or a Mach number, M_n, of about 2. The density jump predicted by the classical theory of shock waves (Landau & Lifshitz 1987) is:

$$\frac{\rho_2}{\rho_1} = \frac{(\gamma + 1)M_n^2}{(\gamma - 1)M_n^2 + 2} \qquad (3)$$

taking $\gamma = 5/3$ and $M_n = 2$, the resulting density jump is 2.3, not much different to the SPH result $\rho_2/\rho_1 = 2.1$ at $t = 250$ s, as can be deduced from Fig. 3. The shock wave is strong at early times but it becomes weaker as the wave goes through the positive density gradient of the secondary. Radiative losses also tend to damp the shock, especially at the beginning, when the Mach number is higher. Nevertheless, the radiated energy is only a small fraction of the internal and kinetic energy of the shocked gas. We have estimated that even though radiative losses are large at the very beginning, when the external piston is still working, they remain well below 10% of the energy deposited by the wave once the shock was born. In addition, the radiated energy is not lost by the star, owing to the small mean free path of the photons. Therefore, the main effect of radiative losses is to slightly redistribute the energy deposited by the wave. We have neglected them in a first approximation. Once this stage was completed, a great deal of the original kinetic energy carried by the ejecta was spread through the secondary by the shock wave. At the same time, direct momentum transfer from the impacting gas to the secondary and the rocket effect due to the ablation imparted a radial velocity of about 50 km s^{-1} to the centre of mass of the remaining material (in the rest frame of the neutron star). As a consequence its orbit began to become slightly eccentric. At $t = 1200$ s the mass lost was $\simeq 6\%$ of the low-mass star.

4) in $t_4 \geq 1200$ s a long period ensued in which the excess of internal energy deposited by the shock wave was converted into kinetic. The secondary began to oscillate with radial pulsations while it remained orbiting and losing matter to the nearby neutron star (last five snapshots in Fig. 5). As the expelled material was carrying rotational and orbital angular momentum, part of the debris formed an accretion disc around the neutron star. The secondary finally achieved the curious "galaxy" shape depicted in the last two snapshots in Fig. 5. In our last model, at $t = 15\,049$ s, the low-mass star had completed almost a third of the orbit, lost 30% of its mass and acquired an orbital eccentricity of $\simeq 0.2$.

Unfortunately our computer resources did not allow us to continue the simulation beyond this point. Once the accretion disc began to form, the time-step became too small to follow the phenomenon over a significant fraction of the orbital motion. Nevertheless, the total destruction of the
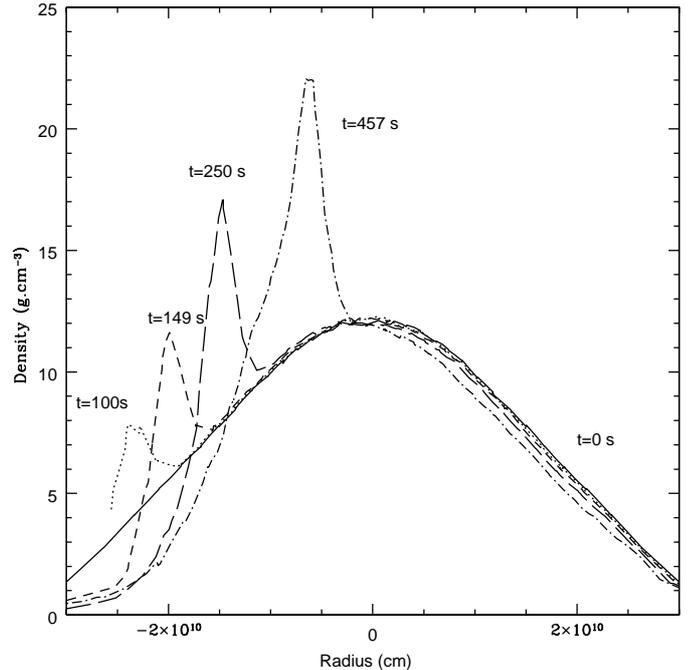

Fig. 3. Density jump caused by the propagation of the shock wave launched by the collision through the secondary star at different times. The continuum line, at $t = 0$ s, is the initial unperturbed profile

secondary is the more probable outcome, as it can be deduced from Fig. 4. This figure depicts the total energy profile and the radius of the secondary at time $t = 15\,049$ s. The Roche lobe radius at this time is $R_L \simeq 4 \ 10^{10}$ cm, which encloses only 0.09 $M_\odot$. At this Lagrangian coordinate the total energy is nearly zero as can be seen in the figure. Therefore, we expect that the secondary will finally disappear after a few orbits, leaving an accretion disc around the compact object.

4. Conclusions

We have carried out a complete simulation of the collision process between the 0.1 $M_\odot$ of gas ejected during the accretion-induced collapse of a white dwarf and a low-mass star (0.3 $M_\odot$). The calculation was done in three dimensions using an SPH hydrocode, which allowed us to incorporate both the orbital elements of the compact binary and the gravitational force exerted by the neutron star. The *main result* of our work is that the combination of the strong collision with the pulling force toward the compact object is able to completely destroy the secondary star, leaving the neutron star alone. Taking into account that the progenitor white dwarf was spun-up by mass transfer in the previous stage to the collapse, the final outcome of this scenario may be either an isolated millisecond pulsar or a normal field pulsar, if magnetic dipole or gravitational radiation were intense enough to slow down the initially fast rotation.

In the standard explanation of the millisecond pulsars phenomenon, the combination of a very short period and
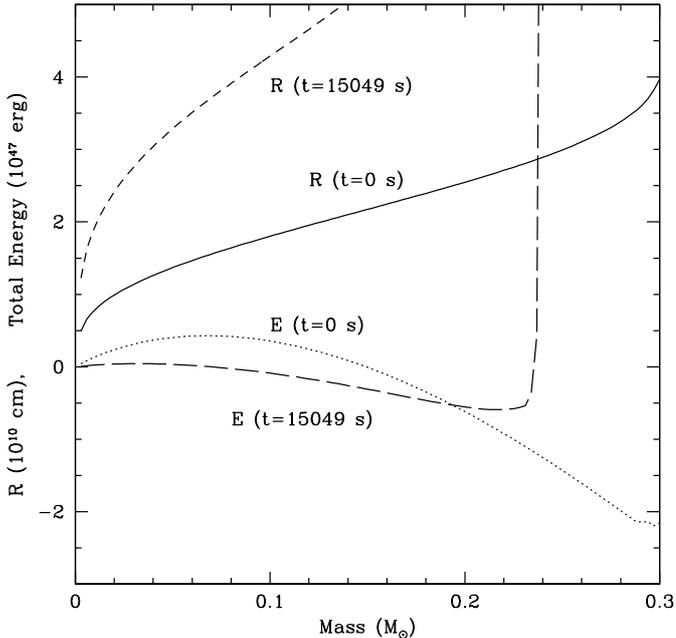
Fig. 4. Total energy profile and radial coordinate as a function of the enclosed mass of the 0.3 $M_\odot$ secondary for both the initial time, $t = 0$ s, and the final time considered, $t = 15\,049$ s.

a small first period derivative is interpreted as an old neutron star (i.e. with low magnetic field) which has been recycled by further mass accretion from the companion star. Nevertheless, in the framework of the AIC of a white dwarf the observed P–Ṗ combination could be addressed if the neutron star were the result of the collapse of a relatively low-magnetized white dwarf which gives rise to a neutron star with a magnetic field $B \leq 10^{10}$ G through flux conservation (Michel 1987; Narayan & Popham 1989). On the other hand, gravitational radiation might be intense after the collapse of the white dwarf, spinning down the pulsar if the neutron star were born without complete spherical symmetry. Small asymmetries could be present at the very beginning due to both, initial eccentricity and internal inhomogeneities formed during the collapse process itself. Quadripolar gravitational radiation induced by eccentricity could be intense at the beginning, but it becomes less efficient as the period increases and rotationally sustained eccentricity rapidly goes down. The resulting braking would probably not be able to take the pulsar out from the millisecond region unless the initial eccentricity were rather large. The amount of gravitational radiation due to the internal instabilities is poorly known. In particular, the so called r-mode instability (Anderson et al. 1999) could be very efficient at removing rotational angular momentum and, if the appropriate conditions are fulfilled, may decelerate the pulsar to a period above 20 ms. Nevertheless, that sort of instability largely relies on pieces of neutron star physics, such as the initial temperature distribution or the details of the cooling rate, which are not yet completely understood. Moreover, neutron stars which are the endproduct of the collapse of ONeMg massive white dwarfs are thought to have lower entropy than

that resulting from the collapse of iron cores of massive stars (Woosley & Weaver 1986). Hence the initial temperature distribution within the neutron star may also be different. Thus, in spite of the aforementioned difficulties of the proposed scenario and given that the standard scenario is not free of problems either, the AIC route to produce steady millisecond rotators cannot be ruled out at present time.

The combination of an accreting massive white dwarf plus a low-mass star (0.3–0.4 $M_\odot$) orbiting in a close orbit with a period of about 0.5 days could, however, be difficult to find in nature. First of all the progenitor binary system must undergo, at least, a common envelope episode in order to shrink the orbit and bring the stars close enough to allow Roche lobe overflow of the secondary. Recently, Sandquist et al. (1998) followed numerically the evolution of binary systems consisting of an asymptotic giant branch star of 5 $M_\odot$ and a 0.4 $M_\odot$ secondary in an initially wide orbit. They concluded that after one common envelope episode a compact binary would emerge consisting of the core of the massive star and the low-mass secondary orbiting at a distance of 4.37 $R_\odot$ with a period of only 0.9 days. Even though the mass of the primary is larger in our case, 10–11 $M_\odot$ in order to get a 1.3–1.35 $M_\odot$ white dwarf, these stars probably undergo an additional common envelope episode related to the carbon shell burning phase (García-Berro & Iben 1994), thus enhancing the possibility of the stars settling into a compact orbit. A second objection is related to the accretion rate from the secondary to the massive white dwarf. As discussed in Sect. 2 the expected rate is rather low, of the order of 10^{-9} $M_\odot$ yr^{-1}, which is currently thought to lead to the total or partial expulsion of the accreted matter due to hydrogen flashes on the white dwarf surface. Nevertheless, owing to the large initial mass of the white dwarf it is necessary to accrete only 0.05–0.10 $M_\odot$ to reach the Chandrasekhar-mass limit. Therefore, even a low effective accretion rate might lead to collapse. In addition, some authors (see, for instance, Fig. 3 of Nomoto & Kondo 1991) claimed that, for massive white dwarfs composed of oxygen, neon and magnesium, very low accretion rates would lead directly to the implosion of the object, due to depressurization induced by electronic captures on ^{20}Ne. The realization frequency of a system consisting of a low-mass star in close orbit around a massive ONeMg white dwarf is not incompatible with the rate of formation of isolated millisecond pulsars. The formation rate in the first case is roughly $\nu_{\rm ONeMg} \simeq 7.6 \; 10^{-4} \, q$ yr^{-1} (Iben & Tutukov 1984), where $q = M_2/M_1$, is the main sequence mass-ratio of the two components. Taking $M_1 = 10$ $M_\odot, M_2 = 0.4$ $M_\odot$ and, considering the difficulties faced by the white dwarf to grow in mass owing to the involved accretion rates, we would expect that $\nu_{\rm ONeMg} < 3 \; 10^{-5}$ yr^{-1}. A rough lower limit for the isolated MSP formation rate can be inferred from Lorimer (1997), who studied the formation rate of 16 low-mass binary pulsars in the solar neighbourhood, three of them isolated MSP, and gave a lower limit for that rate. Restricting his same analysis just to these three pulsars we
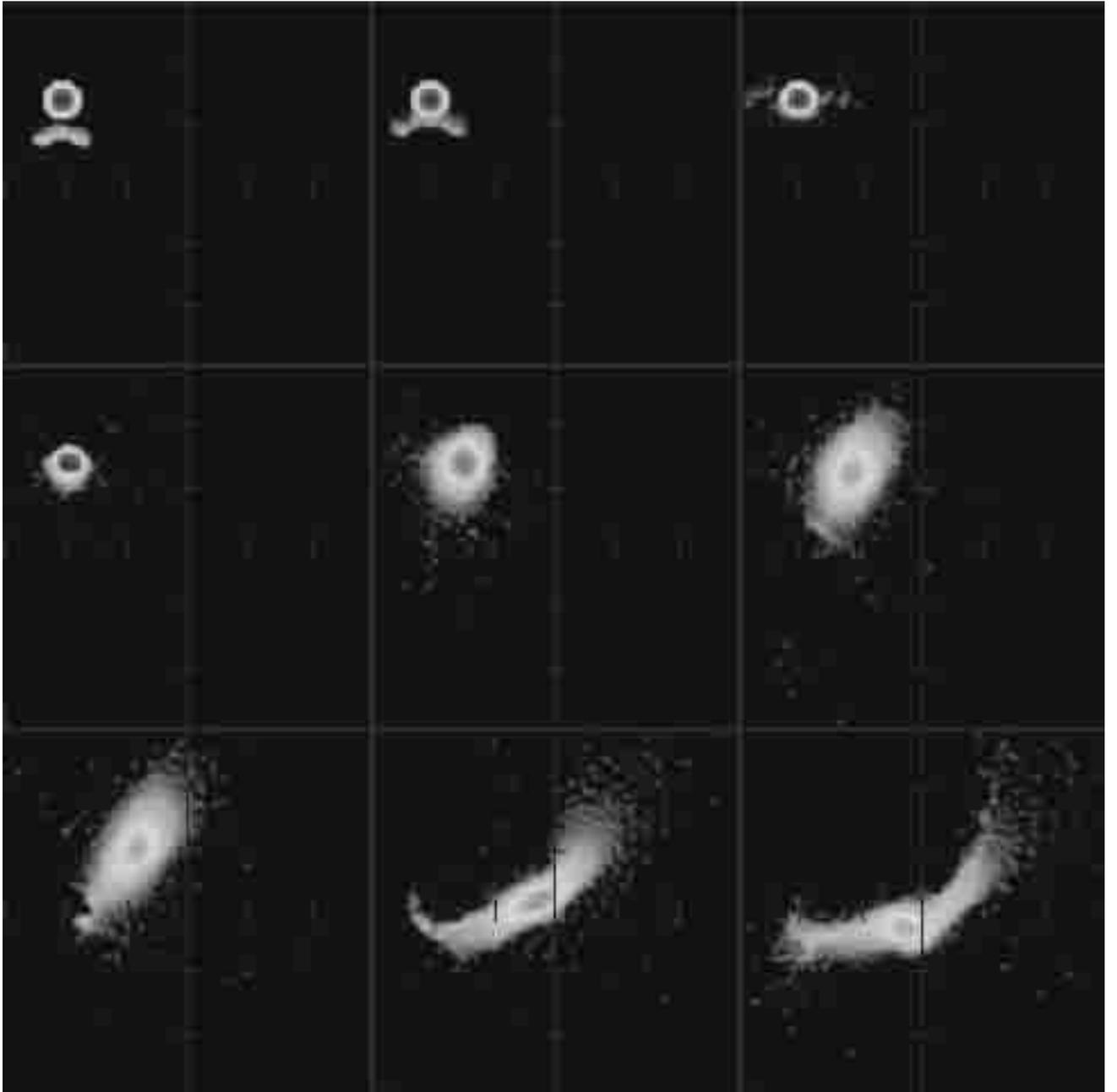
Fig. 5. Evolution of the interaction between the blast wave and the low-mass star. The brightness is proportional to the logarithm of the density. Although the neutron star cannot be seen it is located at the centre of curvature of the ejecta at $t = 0$ s (first snapshot), remaining there throughout the process. The elapsed time is $t = 0$ s, 45 s, 149 s, 513 s, 2467 s, 4337 s, 6257 s, 12 240 s and 15 048 s respectively

infer $\nu_{\mathrm{MSP}} \geq 3\ 10^{-7}$ yr^{-1}. Thus, in view of the large factor between these two limits, it would be enough that one among a few dozens of massive accreting ONeMg white dwarfs reached the Chandrasekhar-mass limit to explain the observed population of isolated millisecond pulsars

Regardless of the way the compact binary has finally formed, the result of our simulation gives an alternative mechanism to the evaporative irradiation of the secondary in order to get an isolated pulsar. Moreover, different explosion strengths could destroy the secondary only partially, leaving very low-mass remnants orbiting around the central pulsar.

References

Anderson, N., Kokkotas, K., & Schutz, B. F. 1999, ApJ, 510, 846

Bhattacharya, D. 1996, in Compact Stars in Binaries, ed. J. V. Paradjis, E. P. J. van den Heuvel, & E. Kuulkers (Dordrecht: Kluwer), 243

Canal, R., Isern, J., & Labay, J. 1990, ARA&A, 28, 183

Chabrier, G., & Baraffe, I. 1997, A&A, 327, 1039

Colgate, S. 1970, Nature, 225, 247

Fryxell, B., & Arnett, D. 1981, ApJ, 243, 994

García-Berro, E., & Iben, I. 1994, ApJ, 434, 306

Gutiérrez, J., García-Berro, E., Iben, I., et al. 1996, ApJ, 459, 701

Hernsquitz, L., & Katz, N. 1989, ApJS, 70, 419

Iben, I., & Tutukov, A. 1984, ApJS, 54, 335

Landau, L. D., & Lifshitz, E. M. 1987, Fluid Mechanics (Oxford: Pergamon)

Livne, E., Tuchman, Y., & Wheeler, J. C. 1992, ApJ, 399, 665

Lorimer, D. R. 1996, in Compact Stars in Binaries, ed. J. V. Paradjis, E. P. J. van den Heuvel, & E. Kuulkers (Dordrecht: Kluwer), 235

Marietta, E., Burrows, A., & Fryxell, B. 2000, ApJS, 128, 615

Michel, F. C. 1987, Nature, 329, 310

Nauenberg, M. 1972, ApJ, 175, 417

Narayan, R., & Popham, R. 1989, ApJ, 346, L25

Nomoto, K., & Kondo, Y. 1991, ApJ, 367, L19

Patterson, J. 1984, ApJS, 54, 443

Ritter, H. 1985, A&A, 148, 207

Ruderman, M., & Shaham, J. 1985, ApJ, 289, 244

Ryba, M. F., & Taylor, J. H. 1991, ApJ, 380, 557

Sandquist, E. L., Taam, R. E., Chen, X., Bodenheimer, P., & Burket, A. 1998, ApJ, 500, 909

Woosley, S. E., & Weaver, T. A. 1986, ARA&A, 24, 205